NISTIR 6353

Preparation and Characterization of Polymer/Dendrimer Blends Progress Report

Eric J. Amis
Barry J. Bauer
Franziska Grohn
Ty J. Prosa
Dawei Liu
Kathleen A. Barnes
Catheryn J. Jackson
Brent D. Viers
Alamgir Karim
Jack F. Douglas

U.S. DEPARTMENT OF COMMERCE
Technology Administration
National Institute of Standards
and Technology
Polymers Division
Gaithersburg, MD 20899, U.S.A

NIST

NISTIR 6353

Preparation and Characterization of Polymer/Dendrimer Blends Progress Report

Eric J. Amis
Barry J. Bauer
Franziska Grohn
Ty J. Prosa
Dawei Liu
Kathleen A. Barnes
Catheryn J. Jackson
Brent D. Viers
Alamgir Karim
Jack F. Douglas

U.S. DEPARTMENT OF COMMERCE
Technology Administration
National Institute of Standards
and Technology
Polymers Division
Gaithersburg, MD 20899, U.S.A

July 1999

U.S. DEPARTMENT OF COMMERCE
William M. Daley, Secretary

TECHNOLOGY ADMINISTRATION
Gary R. Bachula, Acting Under Secretary
for Technology

NATIONAL INSTITUTE OF STANDARDS
AND TECHNOLOGY
Raymond G. Kammer, Director

Table of Contents

General Information 3

Dendrimer Interpenetrating Polymer Networks 4

Ternary Dendrimer Blends..... 7

SANS of Polystyrene Hypergrafts..... 11

Fatty Acid Modified Dendrimer Blends and Solutions..... 15

SAXS of Dendrimer Internal Structure 19

Dendrimers as Crosslink Points in Networks..... 23

SANS of PAMAM-Deuterated Benzoic Acid Solutions..... 26

SANS of PAMAM-PEG Solutions 30

Dendrimer Gold Colloids 33

Gold Filled Fatty Acid Modified Dendrimers 36

Dewetting of Hypergraft Thin Films 38

General Information

Throughout this report certain conventions will be used when describing uncertainties in measurements. Plots of small angle scattering data have been calculated from circular averaging of two dimensional files. The uncertainties are calculated as the estimated standard deviation of the mean and the total combined uncertainty is not given as comparisons are made with data obtained under the same conditions. In cases where the limits are smaller then the plotted symbols, the limits are left out for clarity. In data plots with uncertainties larger than the symbols, representative confidence limits are plotted at appropriate places. Fits of the scattering data are made by a least squares fit of the data giving an average and a standard deviation to the fit, this is true for fit values such as radius of gyration and exponents. Temperatures are given as expected ranges of values based on previous work.

All concentrations are calculated from weighed samples and are reported as mass fractions and are nominal values for naming purposes. The range of the concentrations calculated from mass are within one percent of the reported value. The conventional notation "molecular weight" has been replaced by "relative molecular mass" in most cases. Rarely, the conventional notation is used to conform to previous publications.

Certain commercial materials and equipment are identified in this paper in order to specify adequately the experimental procedure. In no case does such identification imply recommendation by the National Institute of Standards and Technology nor does it imply that the material or equipment identified is necessarily the best available for this purpose.

This work is supported in part by the U.S. Army Research Office under contract number 35109-CH.

Dendrimer Interpenetrating Polymer Networks

NIST: Barry J. Bauer, Ty J. Prosa, Dawei Liu, and Eric J. Amis

Outside Collaborators: Donald Tomalia, MMI, Rolf Scherrenberg, DSM

Objectives:

To synthesize and characterize interpenetrating polymer networks (IPNs) containing dendrimers that are molecularly dispersed.

Technical Description:

Use IPN techniques to prepare molecularly dispersed moderate to large size poly(amido amine) (PAMAM) and polypropyleneimine (PPI) dendrimers in a polymeric matrix. Use small angle xray scattering (SAXS) to measure the radius of gyration of dendrimers and the correlations between dendrimers.

Summary Report:

The IPNs were prepared by dissolving the dendrimers in 2-hydroxyethylmethacrylate (HEMA) containing approximately mass fraction 1 % ethylene glycol dimethacrylate with AIBN as an initiator. They were polymerized at 35 °C for 72 h and at 70 °C for an additional hour.

Figure 1a shows the scattering from solutions and IPNs of PAMAM dendrimers. All SAXS curves show higher order features in the scattering, characteristic of their sphere-like shapes. The positions of these features can be used to estimate the size of the dendrimers, even at high concentration. In going from mass fraction 1 % to mass fraction 26 % in methanol, a peak at low q ($q \approx 0.04$ Å^{-1}) appears. This is due to the correlation formed between the positions of the dendrimers. It has been shown that this is due to the tendency of the dendrimers to avoid overlapping. The positions of the higher order features do not shift, however. This suggests that the dendrimer size remains constant in this concentration range. This has been seen before in poly(propylene imine) dendrimers

.

For the IPNs, the mass fraction 1 % dendrimer sample is quite similar to that of the solution. The second higher order feature of the IPN is difficult to distinguish due to the weak scattering of this sample. As one goes to a mass fraction 10 % dendrimer IPN, the higher order features are shifted to higher q. This indicates that the dendrimer size has decreased. This shifting is also present for mass fraction 10 % and mass fraction 25 % IPNs of G6 and G11. These concentrations are below the overlap concentration of the dendrimers themselves, suggesting that the presence of polymer instead of solvent promotes the shrinkage of the dendrimers.

Figure 1b is a plot of the R_g of dendrimers in solution and in IPNs for G6 through G11 dendrimers. At mass fraction 1 % dendrimer concentration, the R_g values for solutions and IPNs are nearly identical, but there is a significant decrease in R_g of the dendrimers at mass fraction 10 % loading of the IPNs. The dendrimers in IPNs at high concentrations have segment density near that of a bulk PAMAM dendrimer without solvent.

IPNs made by polymerizing a network around linear chains are strongly pushed towards phase separation. It has been shown that when the network size becomes smaller than the linear chain size, the linear chains contract in size and eventually form large clusters. The difference may be related to the very compact, spherical size of the dendrimers. They seem to shrink in size, but remain molecularly dispersed in the polymeric matrix.

Future Plans:

To further investigate these IPN's by synthesizing the PHEMA type with metals incorporated inside the dendrimers by doing the synthesis with metal containing dendrimers and by taking preformed IPNs and exposing them to aqueous metal solutions. To synthesize networks with chains attached to dendrimer crosslink points.

Ternary Dendrimer Blends

NIST: Barry J. Bauer, Dawei Liu, Catheryn L. Jackson, and Eric J. Amis

Outside Collaborators: Aissa Ramzi, DSM, Rolf Scherrenberg, DSM

Objectives:

To measure the effect of hydrophobically modified dendrimers on the miscibility of a polymer blend. To measure the dispersion of the dendrimer in the blend.

Technical Description:

Ternary blends of polystyrene-d (PSD) and poly(vinylmethyl ether) PVME are modified by incorporation of between mass fraction 1 % and mass fraction 10 % dendrimer. SANS is used to locate the phase boundaries and TEM is used to measure the size and dispersion of the dendrimer.

Summary:

As reported previously, hydrophobically modified dendrimers were synthesized from a G5 poly(propylene imine) (PPI) dendrimer with -NH_2 terminal groups by 80 fold mass excess 1,2-epoxy octane in vacuum at 140°C for 8 h. Blends of PSD and PVME were made by mixing in toluene. Solid samples suitable for scattering were prepared by pressing the vacuum dried, powdered blend into disks. SANS from blends with and without added dendrimer demonstrate that the presence of the dendrimer gives the sample stability, causing it to remain miscible when blends without the dendrimer phase separate.

Experiments were continued with G5 PPI dendrimers that were modified by reaction with stearic acid, forming amide bonds on all 64 terminal amino groups. Figure 2a shows the SANS from PSD/PVME = 1/9 (mass ratio) blends with and without mass fraction 1 % of the dendrimer added. Two types of dendrimer were used, one with deuterated stearic acid ($-d_{35}$) and one with hydrogenated stearic acid ($-h_{36}$). At 140 °C, all three samples have scattering typical of a miscible blend. At 150 °C, however, the blend without dendrimer showed increased scattering at low q indicating phase separation is taking place. The blends with the dendrimer still showed scattering typical of micibility at 150 °C. These results are qualitatively similar to previous results of PSD/PVME blends with 1,2-epoxy octane modified dendrimers.

Experiments were repeated under experimental conditions that gave results extending to lower values of q. Figure 2b shows SANS of blends of PSD/PVME = 1/9 (mass ratio) and PSD/PVME = 3/7 (mass ratio) containing mass fraction 1 % of dendrimer. The data were taken at 70 °C which is well within the range of miscbility for the blend without dendrimer. At lower q there is an upturn in the scattering which is typical of a large dispersed phase. The q range shown in figure 2a gives a linear relationship, but when

lower q is probed, the 2 phase structure is evident.

The PSD/PVME 1/9 (mass ratio) samples, ED-1 and ED-4 (containing mass fraction 1 % to 10 % epoxy octane modified G5 DSM dendrimer), were ultramicrotomed to a thickness of ≈60 nm to 80 nm at -70 °C and transferred to 200-mesh, carbon coated Cu grids. The sections were stained with OsO_4 vapors by exposing the grids to a mass fraction 0.04 % aqueous solution of OsO_4at room temperature for 2 h. The blend samples were imaged by transmission electron microscopy (TEM) at 120 kV in a Philips 400T using low-dose conditions.

Figure 2c is the TEM result of ED-1. It shows dark domains of sizes <100 nm, presumed to be aggregates of the dendrimers in the single phase, PS/PVME blend. A PS/PVME 1/9 (mass ratio) blend without dendrimer was examined as a control and did not contain any similar domains; this control sample showed a single phase morphology. ED-4 (mass fraction 10 % dendrimer) contained dark domains of larger and more varied sizes, from 100 nm to 1.0 μm, also presumed to be the dendrimer aggregates.

Therefore, while the dendrimer promotes miscibility of the PSD/PVME, it is not itself miscible with them. The cause of the effect is not known. It may be that a small amount of dendrimer does enter the PSD/PVME phase.

Future Plans:

TEM will be done on a ternary blend that has phase separated thermally and then is quenched. Selective staining of the dendrimer will be attempted to see if it is at the interface or in a separate phase.

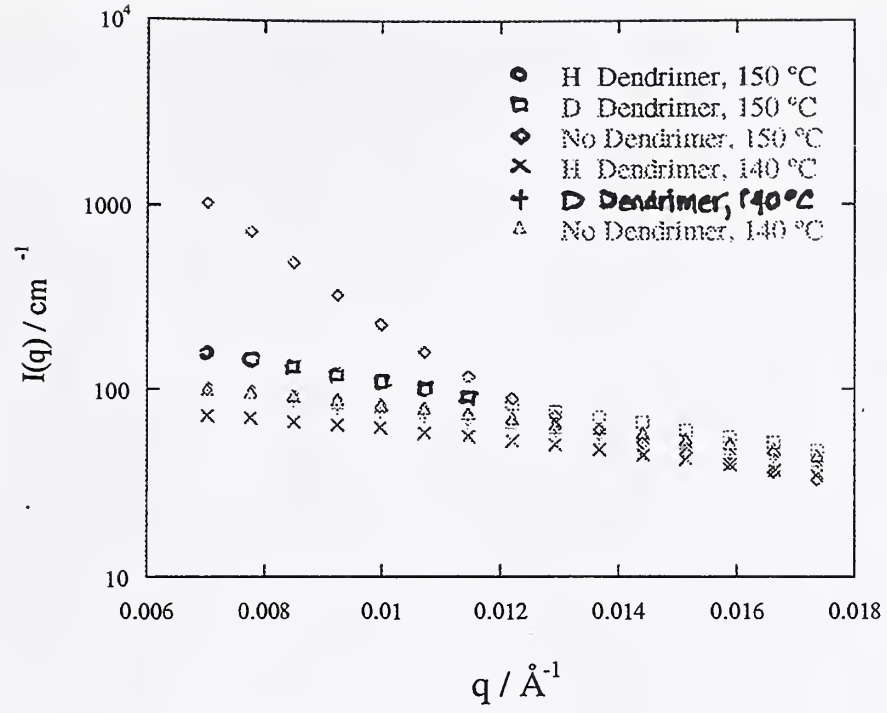

Figure 2a. SANS of PSD/PVME = 1/9 with and without mass fraction 1 % dendrimer at 140 °C and 150 °C.

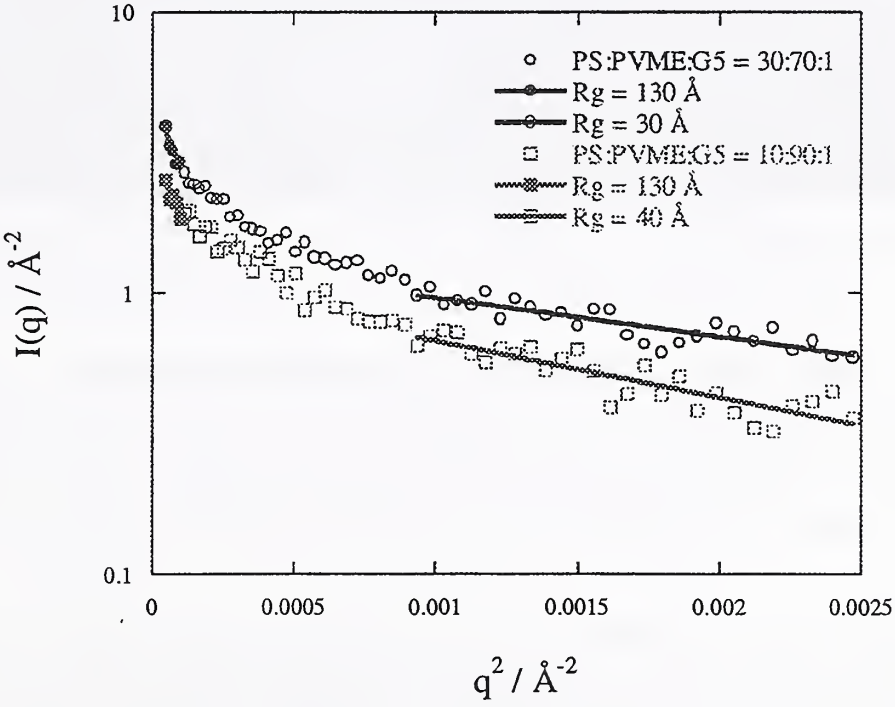

Figure 2b. SANS of PSD/PVME = (1/9 and 3/7) with and without mass fraction 1 % dendrimer at 70 °C.

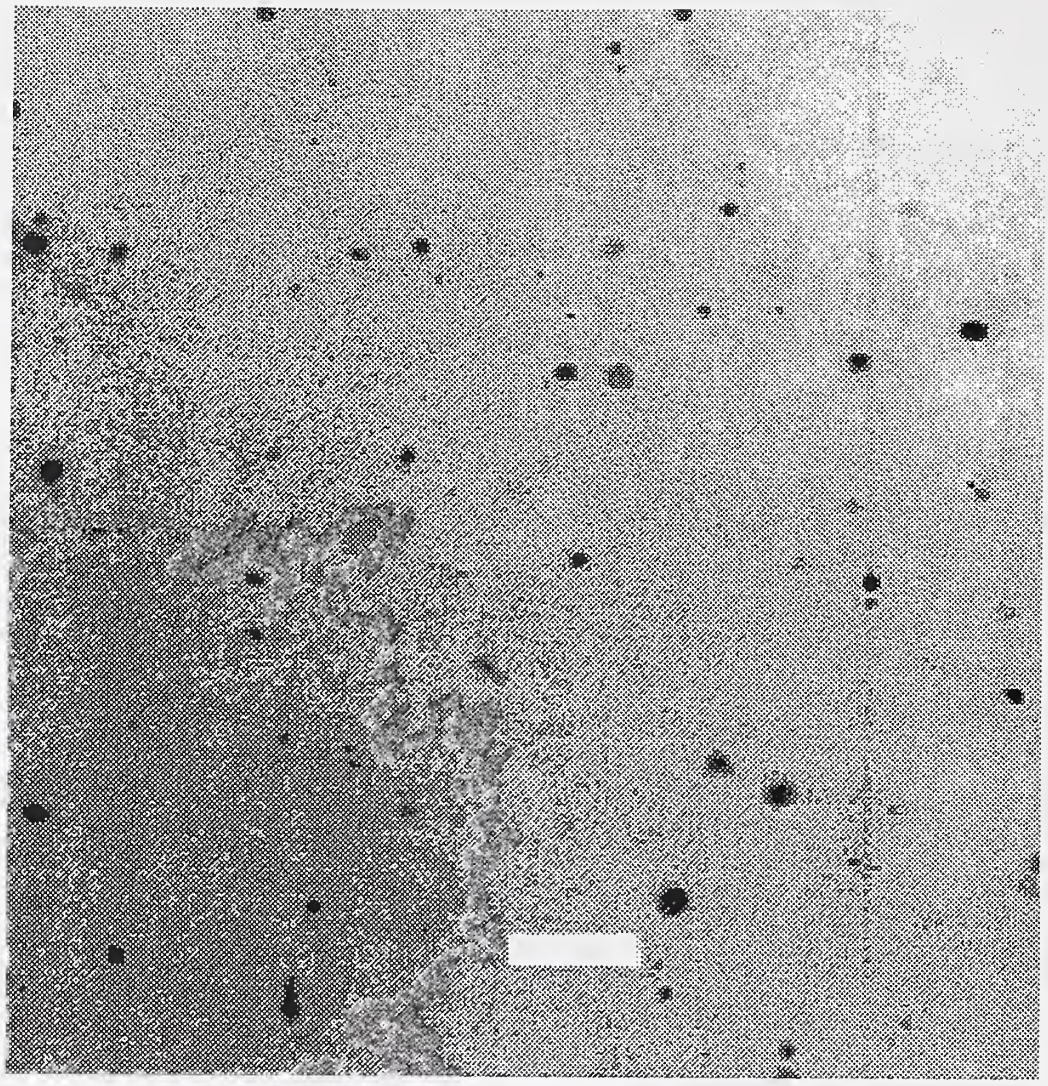

Figure 2c. TEM of PSD/PVME blend ED-1. The scale bar is one mircon.

SANS of Polystyrene Hypergrafts

NIST: Andreas Topp, Barry J. Bauer

Outside Collaborators: Mario Gauthier, U. Waterloo, S. Choi, U. Maryland, Robert M. Briber, U. Maryland.

Objectives:

To measure the size and interaction parameters of polystyrene (PS) hypergrafts in blends with linear PS and poly(vinylmethyl ether) (PVME).

Technical Description:

Use SANS to measure the radius of gyration of PS hypergrafts generations G0 to G3 in blends with linear PSD and to determine the effect of branching on the miscibility.

Summary Report:

Dendrigraft or aborescent graft polymers are branched macromolecules synthesized by successive cycles of functionalization and grafting reactions. The molecules discussed here are synthesized from polystyrene grafted onto a polystyrene backbone. Grafting linear polystyryl anions onto a partially chloromethylated linear polystyrene yields a generation 0 polymer and repetition of the chloromethylation and anionic grafting reactions gives higher generations. The grafting sites are believed to be distributed randomly throughout the molecule. The structure of arborescent graft polymers are related to dendrimer molecules, but since the building blocks are polymer chains rather than monomers, arborescent graft polymers with very high molecular mass can be obtained within a few generations. Since the branching in aborescent polymers is very dense, the distribution of graft sites becomes uniform throughout the molecule.

A Guinier fit of the data gives R_g values of the molecules in solvents or blends. Figure 3a gives the R_g of various generations. The sizes are not strongly affected by solution or blend type until G3. The sizes of the G3 change as toluene > cyclohexane > PVME > PS which follows the strength of interaction with the more favorable Flory Huggins interaction parameter, χ, giving the largest sizes, and solutions giving larger sizes than blends.

Figure 3b shows the scattering from the G3 polymer in PVME-d3 at various temperatures. At low temperatures, the size remains constant and the molecules are well dispersed, but at 115 °C there is a transition producing an additional peak at low q. This indicates that there is a phase separation, with the hypergrafts coming together but not interpenetrating. The shifting of the higher order features to higher q indicates that the hypergrafts are collapsing when they phase separate.

The SANS data for generation 3 polymers shows a clear Guinier region and a second interference peak at higher q. This second peak is characteristic of single particle with relatively uniform density. Attempts to fit the data for generation 3 in both deuterated cyclohexane and deuterated toluene using a simple model such as hard sphere were not successful. Scattering curves calculated for various core/shell models (with lower density in the interior of the molecule as suggested by de Gennes and Hervet) actually fit the data worse with calculated scattering lying significantly above that for the hard sphere model. As an alternative model a power law density function was used to fit the data. The equation used was:

$$\rho(r) = 1 - \left(\frac{r}{R_{max}} \right)^{\alpha}$$

where R_{max} corresponds to the maximum outside radius. When α goes to infinity this model is equivalent to a hard sphere model.

Figure 3c plots the segment density distributions that gave the best fits of the scattering. The distributions show that for the best solvent, toluene, the molecules are extended to their greatest size and have the largest zone of transition at the outside. There is a continuous shrinkage with decreasing interactions (increasing χ) until the G3 molecules collapse to near bulk density in PS. Even though the G3 molecules are collapsed in the PS matrix, they still are well dispersed and do not show signs of aggregation.

Future Plans:

Blends will be made at higher arborescent polymer concentrations and SANS will be used to see if ordered structures will formed.

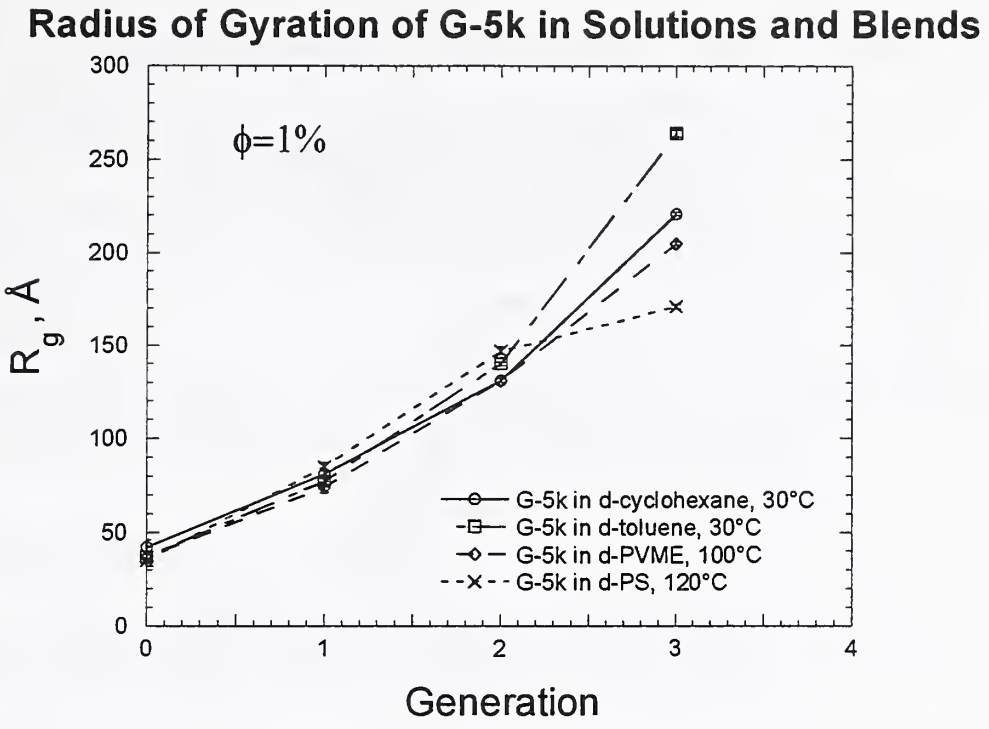

Figure 3a. Rg of hypergraft PS G0, G1, G2, G3 in solutions and blends.

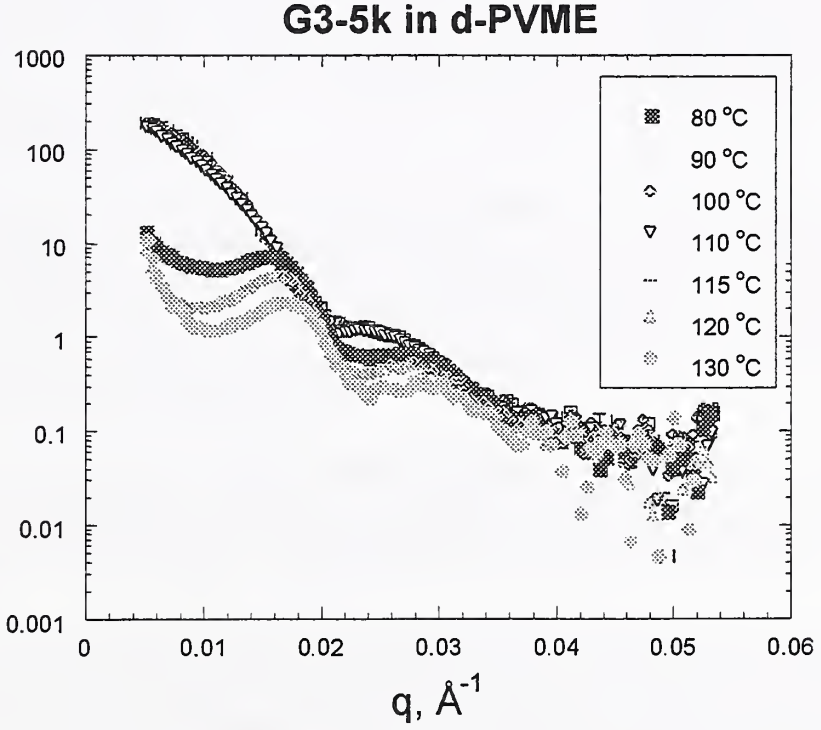

Figure 3b. SANS of G3 hypergraft PS in PVME.

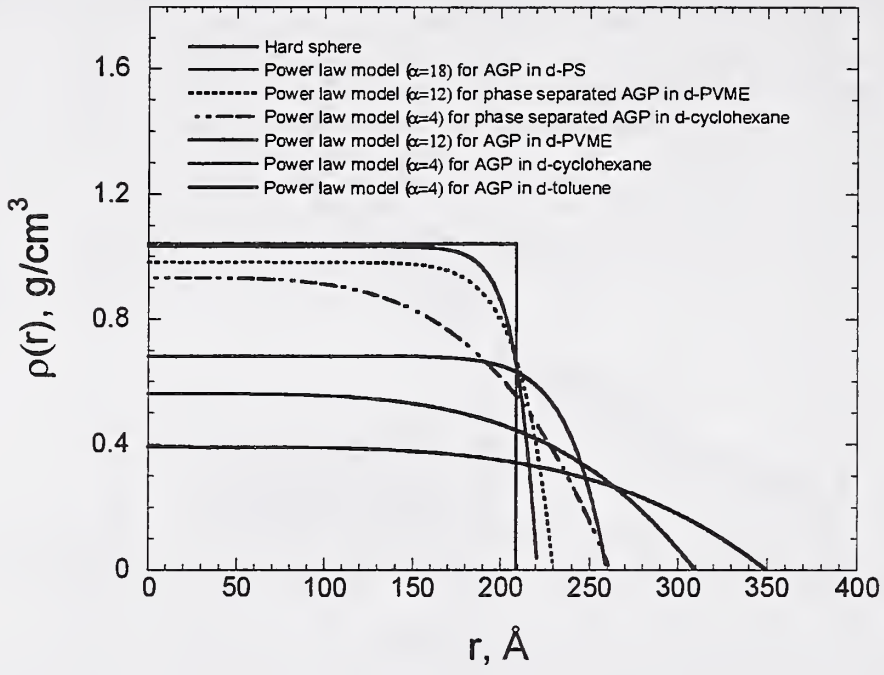

Figure 3c. Segment density distributions of hypergraft G3 in solution and blend from the SANS results.

Fatty Acid Modified Dendrimer Blends and Solutions

NIST: Kathleen A. Barnes, Barry J. Bauer, Eric J. Amis

Outside Collaborators: Aissa Ramzi, DSM, Rolf Scherrenberg, DSM, Jacques Joosten, DSM

Objectives:

To evaluate the morphology of chemically modified dendrimers in bulk and in solution. To determine if these dendrimers form a miscible blend with polyolefins.

Technical Description:

Use SANS to measure the type and size of the morphology in the bulk. SANS of solutions of dendrimers in aliphatic solvents $CH_3(CH_2)_{n-2}CH_3$ with n = 8, 10, 12, 16, 20, and 24 will be used to measure the effect of chain length on miscibility.

Summary Report:

Fatty acid modified PPI dendrimers (FAD) are being used as vehicles for dispersing dyes into polyolefins. Previous reports have shown that these dendrimers do not disperse on a molecular level, but form aggregates. Figure 4a is a plot of SANS data on mass fraction 2 % mixtures of modified dendrimers G1, G3, and G5 in a HDPE-d4 matrix. The limiting power law of –4 shows that the dendrimers are phase separated into domains of pure dendrimer and PE.

To understand the interaction of FAD with polyolefin polymers, SANS of solutions was done in aliphatic solvents $CH_3(CH_2)_{n-2}CH_3$ with n = 8, 10, 12, 16, 20, and 24 to measure the effect of chain length on miscibility. The dendrimer used was the G5 PPI dendrimer that was esterfied with stearic acid-d35 which gave good SANS contrast with the solvents used. Solutions were made of mass fraction (1, 3, and 5) % and SANS was done at temperatures between 60 °C and 120 °C.

Figure 4b shows the R_g of the dendrimer extrapolated to zero concentration in various solvents and temperatures. There is no significant change in the size of the dendrimers over the whole range, only a subtle shrinkage as the solvent conditions become less favorable.

Figure 4c is a plot of the second virial coefficient, A_2, as a function of solvent conditions. The values of A_2 are negative and have a slight trend to get more negative as the temperature increases. A negative second virial coefficient is characteristic of a very poor solvent, one that is worse than a θ solvent. Apparently the reason the dendrimer remains

in solution is that it has a relatively low molecular mass. Straight chain hydrocarbons are not good solvents for FAD and it is consistent that high molecular weight polyethylene is not miscible with FAD. While dispersion may be at a small size scale, there is no dispersion on a molecular level.

Future Plans:

To form monolayer blend films on surfaces and characterize them by neutron and x-ray reflectivity. Dendrimers with other surface chemistries may be used to vary the blend miscibility.

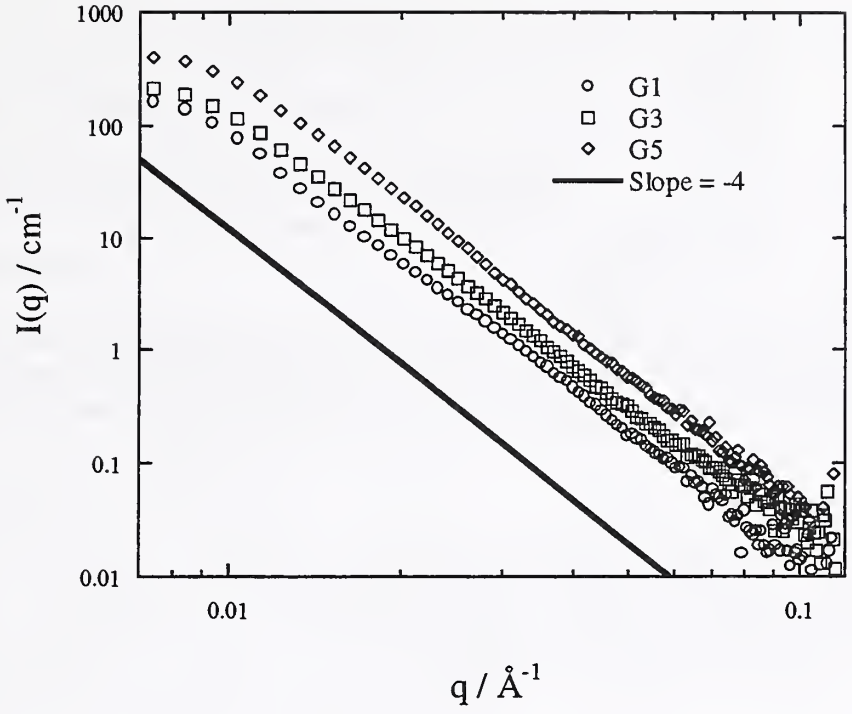

Figure 4a. SANS of mass fraction 2 % FAD in polyethylene-d4, Generations G1, G3, G5.

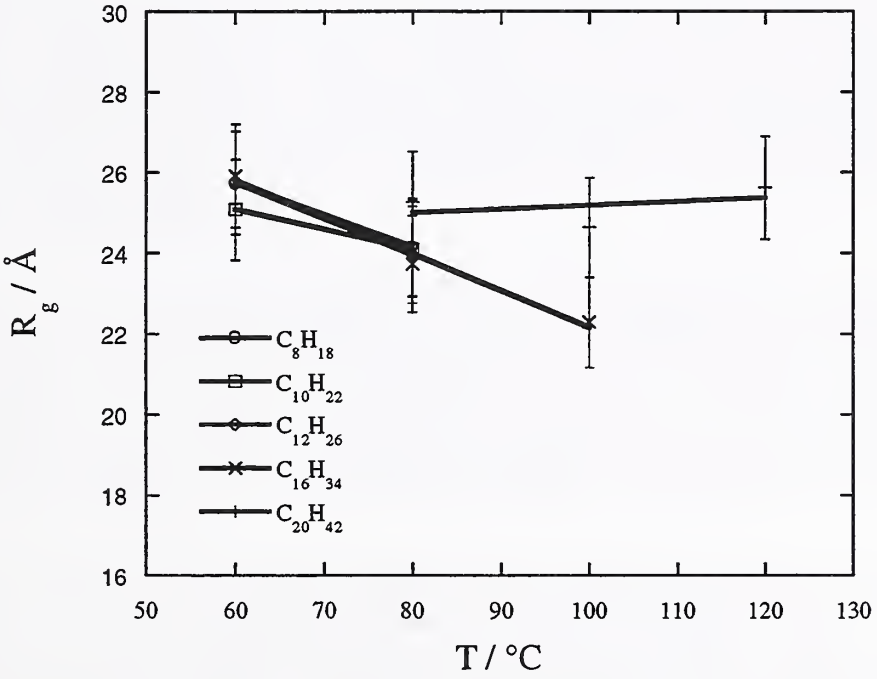

Figure 4b. R_g of FAD-d G5 in hydrocarbon solvents extrapolated to zero concentration.

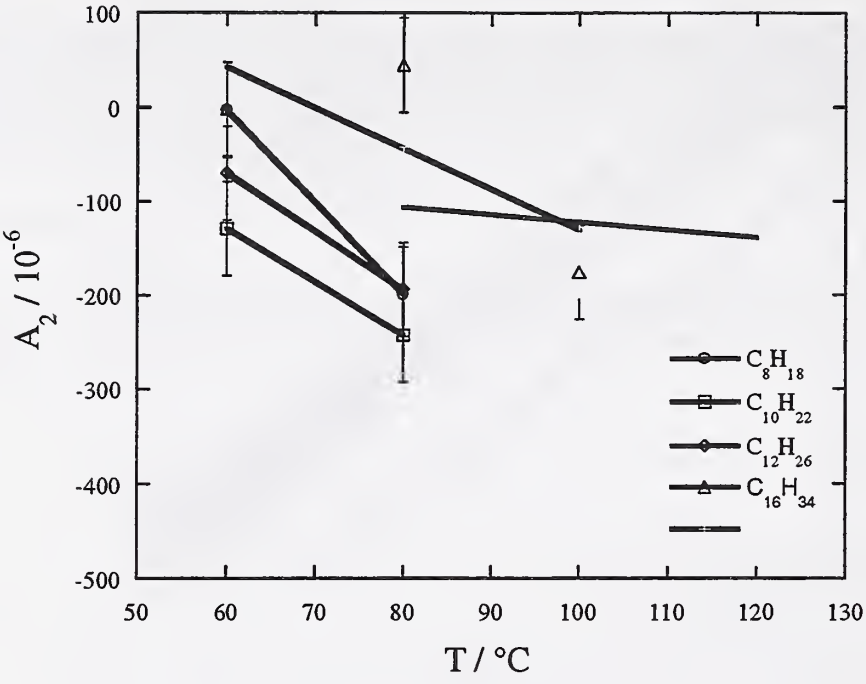

Figure 4c. Second virial coefficient of FAD-d G5 in hydrocarbon solvent.

SAXS of Dendrimer Internal Structure

NIST: Ty J. Prosa, Barry J. Bauer, Eric J. Amis

Outside Collaborators: Donald Tomalia (MMI)

Objectives:

To extract information about intramolecular dendrimer composition from small angle x-ray scattering (SAXS) in order to better assess potential applications. This includes dendrimer size, shape, size dispersity and internal segment density profiles.

Technical Description:

SAXS from dilute solutions of various dendrimers in methanol was investigated at the newly commissioned National Synchrotron Light Source's Advanced Polymers-Participating Research Team (AP-PRT) beamline at the Brookhaven National Laboratory. The combination of high x-ray flux and improved resolution has allowed for experimental data suitable for detailed quantitative analysis.

Summary Report:

SAXS from dilute solutions of dendrimers exhibits scattering features that depend primarily on the intramolecular structure within the individual dendrimers. Previous SAXS studies from this laboratory reported on scattering data of sufficient quality to measure R_g and to suggest that at large generations, dendrimers exhibit additional features consistent with a sphere-like molecular organization. However, these measurements were not sufficient to allow one to distinguish between competing models with varying segment density distributions.

PAMAM dendrimers of generation 3 to 10 (G3 to G10) were prepared mass fraction 1 % solutions of dendrimer in methanol, and data was collected at the AP-PRT beamline. Scattering from generations G3 through G10 are shown in figure 5a as a Porod plot to emphasize the power law scattering at high q. There is a continuous transformation in the scattering over this range. The high q slope is greatest for G3 and levels out as one goes to G10. The larger dendrimers show several higher order features of the scattering typical of spherical objects.

The SAXS of G3 is replotted in figure 5b as a Kratky plot to show the q^{-2} scattering at high q. This is characteristic of scattering from star polymers, both in the limiting q dependence and the peak in the Kratky plot. The theoretical scattering of stars with 14.9 and 33.6 arms are also plotted to give extremes of fits to the high q plateau and the whole q range. The fits are quite poor, demonstrating that the small dendrimers are star-like in certain characteristics, but the overall segment density distribution is quite different from

that of star molecules. Even for the smallest dendrimers measured, the interior of the molecules is much more uniform and the transition on the outside is sharper than for stars.

The scattering from a mass fraction 5 % G10 dendrimer is shown in figure 5c along with the theoretical scattering from different models. Figure 5d shows the segment density distributions that give the lines shown in figure 5c. The shapes of the lines in figure 5d correspond to the three types of fits. The parallel lines to the right of the figure show the limits of the polydispersity, the slopes of the lines at the right show the thickness of the transition zone, and the slope of the upper horizontal lines of the distributions show the relative hollowness.The best fit for a rectangular distribution of spheres gives an average radius of (68.0 ± 0.1) Å with a distribution half width of (6.2 ± 0.1) Å. A rectangular distribution with a width and an outside zone of transition gives an average radius of (67.8 ± 0.1) and an average half width of (6.2 ± 0.1) Å and a transition zone thickness of (3.0 ± 0.2) Å. The third fit floats the segment density at the center and gives a ratio of the center density to the exterior density of (0.98 ± 0.02) Å.

The fits suggest that the G10 dendrimers have a uniform interior without any hollowness. There is a narrow polydispersity of the dendrimer diameters and a very small zone of transition of segment density at the outside.

Future Plans:

To continue to characterize dendrimers from various sources as to their size and homogeneity.

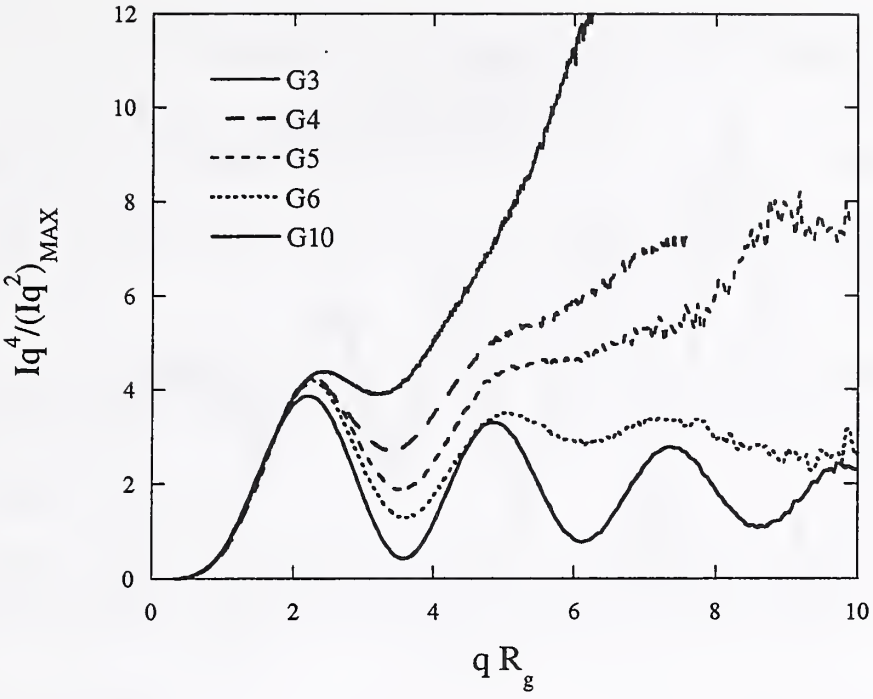

Figure 5a. SAXS Porod plots of PAMAM dendrimers G3, G4, G5, G6, and G10.

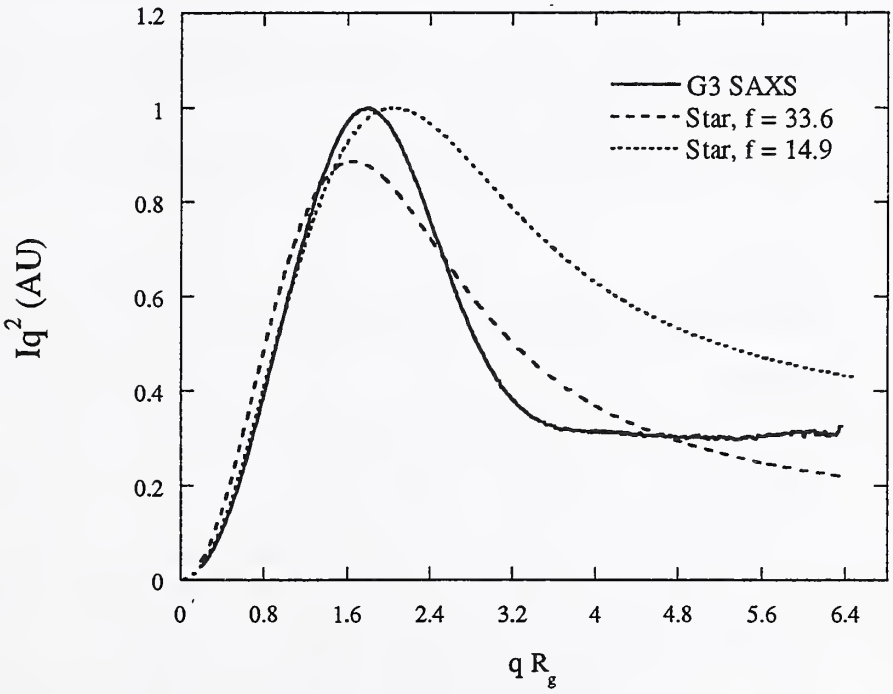

Figure 5b. SAXS Kratky plot of G3 PAMAM dendrimer. Fits of star polymers with 33.6 and 14.9 arms.

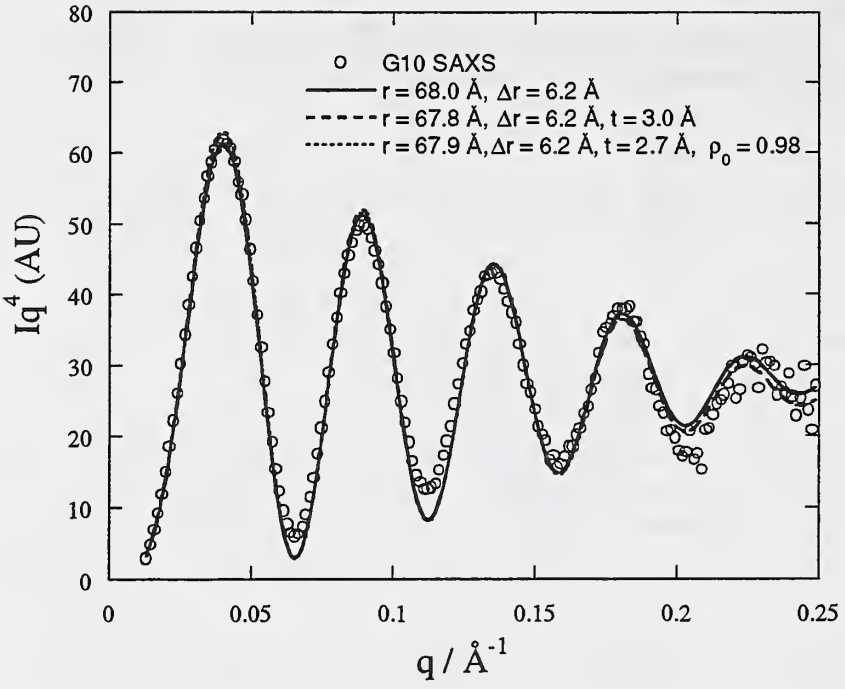

Figure 5c. SAXS Porod plot of G10 PAMAM. Fits for polydisperse spheres, polydisperse spheres with transition zone, and polydisperse spheres with transition zone and hollowness.

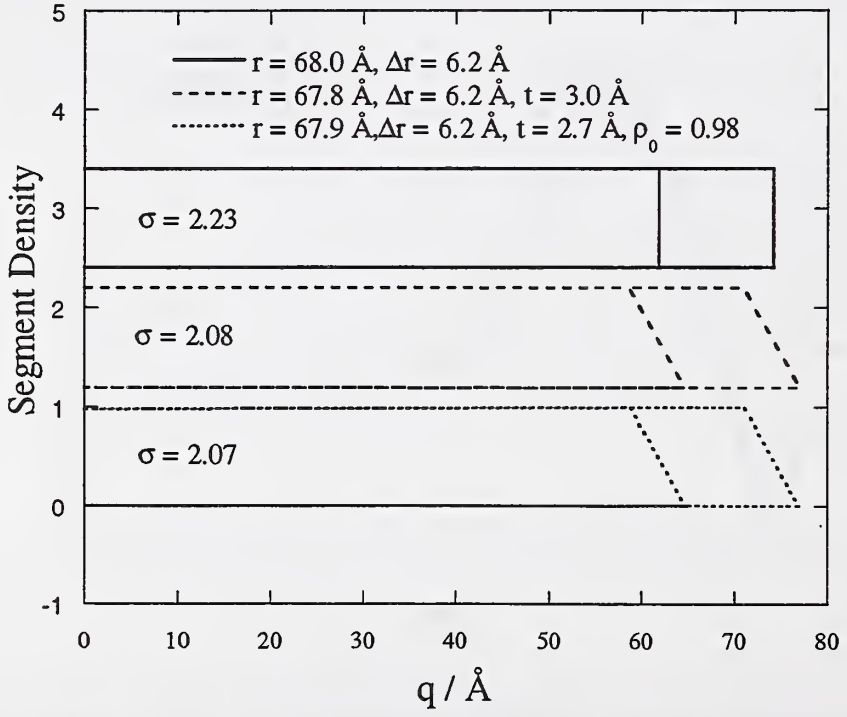

Figure 5d. Segment density distributions shown in fits in figure 5c.

Dendrimers as Crosslink Points in Networks

NIST: Brent D. Viers, Barry J. Bauer, Eric J. Amis

Outside Collaborators: Donald Tomalia (MMI), Rolf Scherrenberg (DSM)

Objectives:

To incorporate dendrimers into a polymeric matrix by using them as multifunctional crosslink points.

Technical Description:

PAMAM and PPI dendrimers having multiple terminal primary amines are reacted with α,ω functionalized linear polymers using Michael addition of acrylates or polyurethane formation with isocyanates.

Summary Report:

We have used the functional amine groups on the periphery of commercially available PAMAM and PPI dendrimers to "end-link" with a complementary functionality on the ends of a linear polymer to form a macromolecular network. The matrix polymer of interest was poly(ethylene glycol), which (like the dendrimer) has the desirable properties of being water soluble, biocompatible, and commercially available in a variety of molecular weights and with a variety of end group chemistries. Thus far, we have successfully formed gels in relatively dilute solution (ca. 10 percent total solids by mass) in polar aprotic solvents such as n-methyl pyrrolidone (NMP) and dimethyl sulfoxide (DMSO).

Variable parameters included the molecular weight (generation) of the dendrimer, which varied from 3^{rd} generation dendrimers having 16 amine groups to 5^{th} generation dendrimers having 64 amine groups; the molecular weight of the poly(ethylene glycol), which spanned nearly an order of magnitude in molecular mass, ranging from 575 g mol^{-1} to 3400 g mol^{-1}; and the molar ratios of the two components. Of even greater interest was the specific endlinking chemistry. For example, an acrylate terminated poly(ethylene glycol) can react via a Michael addition similar to what is used to "grow" successive generations of the dendrimer. Gelation via this Michael addition occurred relatively slowly (ca. hours) to form monolithic, mechanically robust gels. These gels were reasonably elastic, as indicated by the ability to sorb solvent and swell to a reproducible, equilibrium value. Unfortunately, these gels were not hydrolytically stable, and would break apart in protic solutions of water or methanol. We attribute this behavior as resulting from hydrolysis of the ester linkage in the acrylate moiety.

Conversely, we were able to form gels from the reaction of an isocyanate terminated poly(ethylene glycol) with the primary amine, forming an urea linkage. This linkage, as

expected, was hydrolytically stable. However, the gelation reaction was so fast as to be almost instantaneous. While seemingly transparent, the resultant gel tended to be weak.

SANS can be used to follow the crosslinking reaction as is shown in figure 6a. It shows the SANS from a reaction of PEG 3175 diacrylate with PPI G5 at mass fraction 2% solids. The scattered intensity increases with reaction time indicating the buildup of molecular weight as the reaction proceeds. The circles represent the scattering immediately after mixing and the crosses show the final conversion.

Future Plans:

To use other chemistries to do the crosslinking reaction to insure rapid and complete hydrolytically stable bond formation. To characterize the networks by scattering and physical property measurements. To synthesize and characterize networks containing metals and small organic molecules.

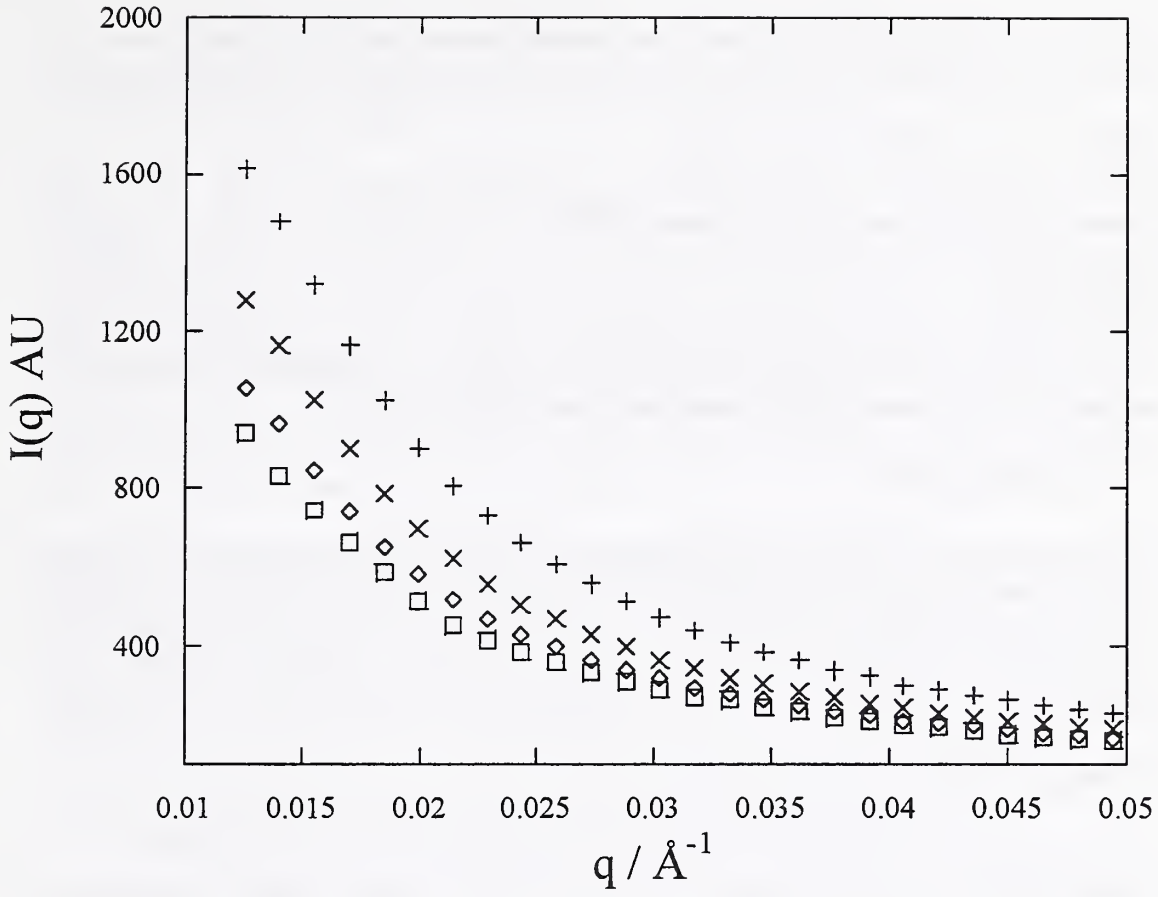

Figure 6a SANS of curing mizture of PEG 3175 diacrylate and PPI G5 dendrimer.

SANS of PAMAM-Deuterated Benzoic Acid Solutions.

NIST: Giovanni Nisato, Eric J. Amis

Outside Collaborators: Donald Tomalia, MMI

Objectives:

Use SANS to assess the ability of PAMAM dendrimers to solubilize guest molecules in aqueous solution through electrostatic or hydrophobic interactions.

Technical Description:

SANS is used on solutions containing various concentrations of deuterated benzoic acid, while keeping the dendrimer (PAMAM G8) content fixed at a fairly low concentration (mass fraction 1 %). The experiments are performed in a solvent matching the contrast factor of the dendrimers, so that variations of the scattering intensity can be unambiguously attributed to the structure factor of the deuterated benzoic acid molecules.

Summary Report:

The samples studied were mass fraction 1 % solutions of Generation 8 PAMAM (MMI. The solvent was a volume fraction 61.8 % H_2O / 38.2 % D_2O mixture. This composition corresponds to the contrast match conditions for PAMAM dendrimers. [1] The molar ratio of deuterated benzoic acid to the number of primary amines carried by the terminal groups of one dendrimer is designated α = [dBenzoic Acid]/[NH_2]. Note that $\alpha = 2$ means that there is one molecule of deuterated benzoic acid for every amine group in the dendrimer, either primary (terminal units) or tertiary (repeat units). The effect of monovalent salt is considered by preparing solutions in the presence of 200 mMol/L of NaCl. It is noteworthy that deuterated benzoic acid is not soluble in water; solubilization occurs upon addition of stock dendrimer solution and stirring (≈10 min). The final pH of different solutions is reported in the table below.

α	pH	pH 200 mMol/L NaCl added
0	-	10.4 ± 0.1
0.3	-	9.3 ± 0.1
0.5	8.3 ± 0.1	8.9 ± 0.1
1	6.2 ± 0.1	6.7 ± 0.1
2	4.3 ± 0.1	4.5 ± 0.1

Figure (7a) is a comparative plot showing scattering intensity of pure D_2O, pure H_2O, the matched solvent, and a mass fraction 1 % PAMAM solution in the matching conditions.

The results clearly show that the solvent matching conditions are satisfied. In this solvent, the dendritic polymer is "masked out" and only the coherent scattering of the deuterated benzoic acid will be detected.

Figure (7b) shows the excess scattering of a mass fraction 1 % dendrimer solution (matched solvent), in the presence of different amounts of deuterated benzoic acid. The scattering profiles are very similar to the one observed in solutions of electrostatically charged dendrimers. The most remarkable feature is the presence of a very pronounced peak (q^*) occurring in the low q range. The amplitude of the scattered intensity correlates well with the amount of deuterated benzoic acid, whereas the actual value of q^* does not depend on this concentration. Rather, it corresponds to the average *inter-dendrimer* distance which can be expected at this dendrimer volume fraction and is in quantitative agreement with the observations of Valachovic.

Figure (7c) shows that, upon addition of monovalent salt, the coherent scattering intensity decreases by several orders of magnitude and becomes practically negligible for $\alpha < 1$. The last data set in Figure (7c), corresponding to $\alpha = 2$, could be fit to a Guinier functional form, yielding an apparent radius of gyration of 46 ± 2 Å, which is comparable to the *radius* of one G8 dendrimer. The samples do not show any signs of macroscopic precipitation of the deuterated benzoic acid, nor does the pH indicate any drastic variations upon addition of salt. Upon addition of NaCl, the deuterated benzoic acid molecules are still in solution, but they are no longer spatially correlated.

It seems that ordering mechanism is essentially electrostatic rather than being driven by hydrophobic interactions between the core of the dendrimer and the deuterated benzoic acid. In the first case [Figure (7a)], these molecules seem to act as counterions statistically localized in the vicinity of the dendrimers. The latter are organized in a liquid-like structure owing to the long-range electrostatic interactions. Upon addition of salt, the electrostatic interactions are screened and the deuterated benzoic acid molecules are in competition with the Cl^- ions in solution which can also as counter-ions for the dendrimers. The spatial correlations between the benzoic acid molecules then decrease dramatically, even though for high loading values ($\alpha = 2$), it seems that these molecules are preferentially located in the immediate vicinity of the dendrimers.

Future Plans:

Study more systematically the effect of α and modify the pH conditions. These studies are necessary to assess the ability of dendrimers to carry and *release* molecules of a more interesting nature, e.g. pharmacologically active. Also, it would be interesting to measure more accurately the spatial distribution of the deuterated markers to find out whether these molecules have access to the interior of the dendrimer structure.

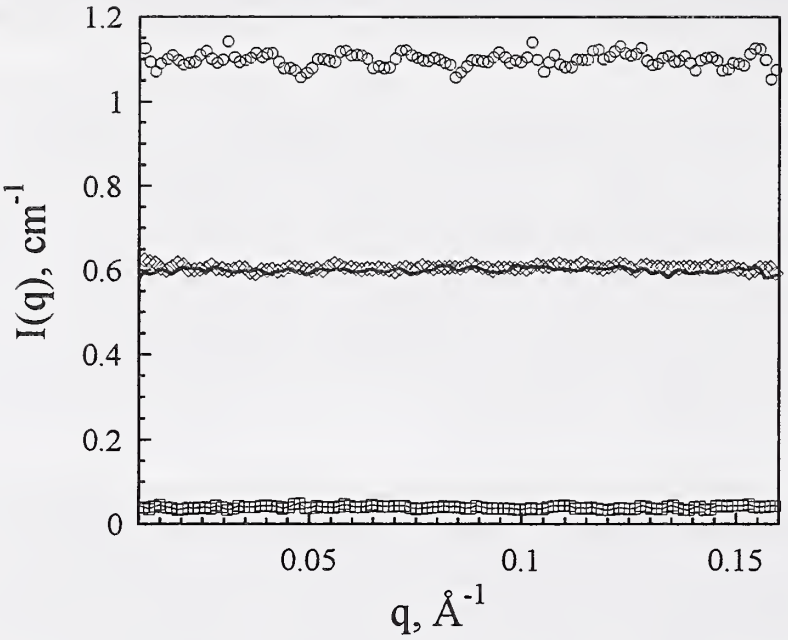

Figure 7a. Comparison of the scattering intensity of pure D_2O (squares), pure H_2O (circles), the matched solvent (continuous line) and a mass fraction 1 % PAMAM solution in matching conditions (diamonds).

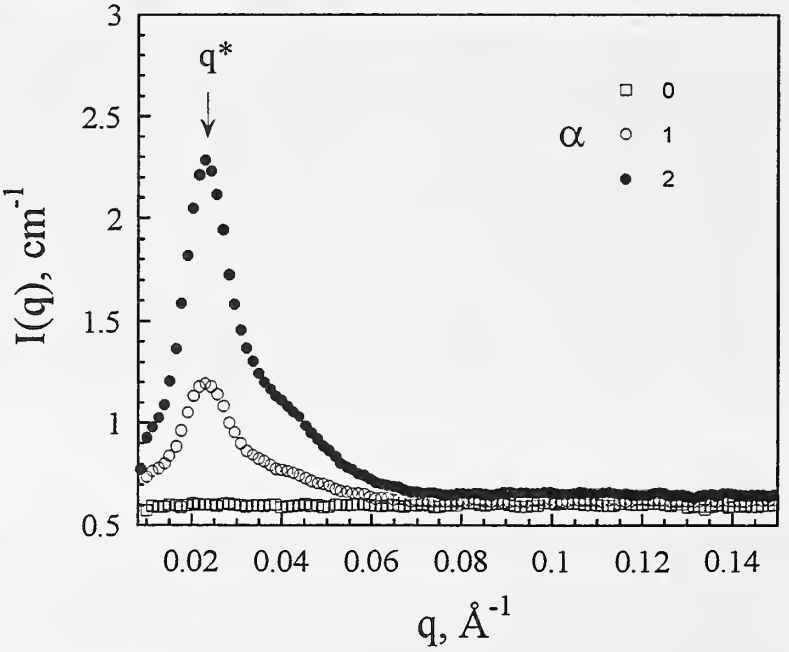

Figure 7b. Excess scattering intensity of mass fraction 1 % PAMAM dendrimer solutions (G8) in matched solvent for various amounts of deuterated benzoic acid (see legend). NB: α = [dBenzoic Acid]/[NH_2].

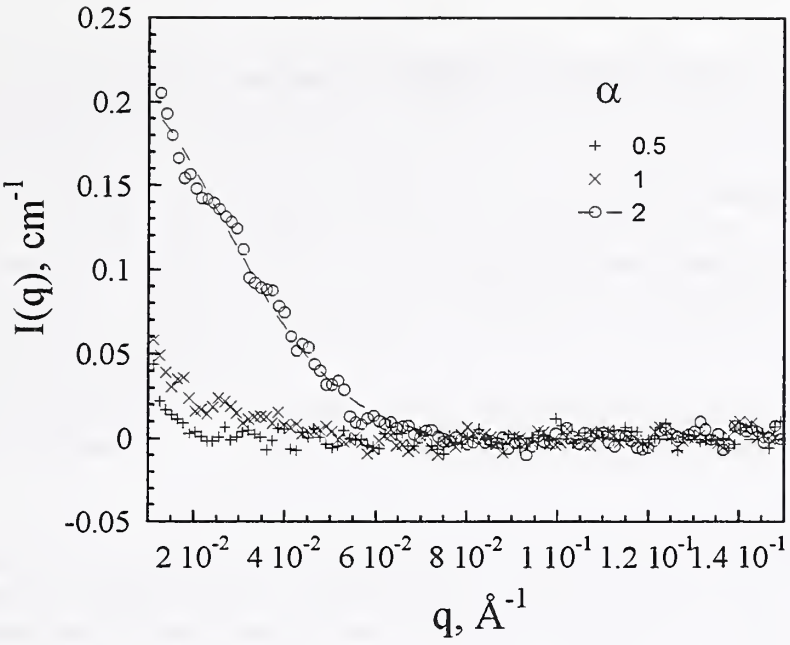

Figure 7c. Excess scattering intensity of mass fraction 1 % PAMAM dendrimer solutions (G8) in matched solvent in the presence of 200 mMol/L NaCl for various amounts of deuterated benzoic acid (see legend). The dashed line is a Guinier fit to the data.

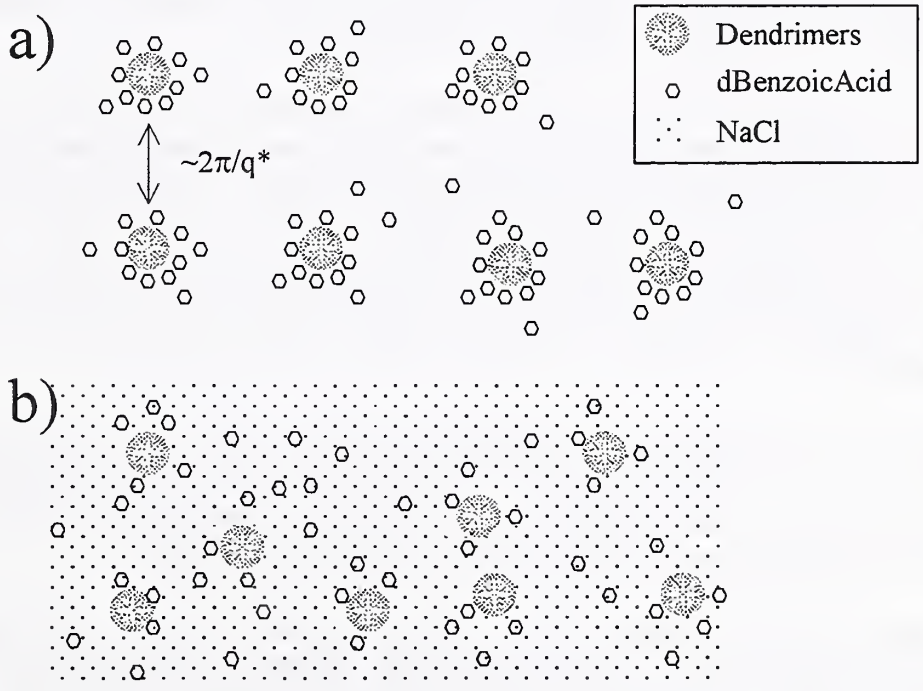

Figure 7d. Illustration of the proposed interpretation. a) No added salt, b) added salt.

SANS of PAMAM-PEG Solutions

NIST: Giovanni Nisato, Eric Amis

Outside Collaborators: Donald Tomalia, MMI.

Objectives:

To use SANS to measure the size variation of PAMAM dendrimers in the presence of the neutral polymer poly(ethylene glycol) (PEG) in aqueous solutions.

Technical Description:

SANS is used on solutions containing various concentrations of PEG, while keeping the dendrimer (PAMAM G8) content fixed at a relatively low concentration. The experiments are performed in a solvent matching the contrast factor of PEG, so that variations of the scattering intensity can be attributed to the dendrimer form and structure factors.

Summary Report:

The samples studied were mass fraction 1 % Generation 8 PAMAM in the presence of various amounts of 18,500 M_r PEG (Polyscience). The samples were dissolved a volume fraction 82.4 % H_2O / 17.6 % D_2O by volume mixture. This composition corresponds to the calculated contrast factor of PEG (matching conditions).

Figure 8a is a comparative plot showing scattering intensity of pure D_2O (squares), mass fraction 15 % PEG in pure D_2O (open circles), the matched solvent (crosses) and a mass fraction 15 % PEG (filled circles) in the matching conditions. The results clearly show that the calculated solvent matching conditions are satisfied. In this solvent, the linear polymer is "masked out" and only the coherent scattering of the dendrimers will shown up. The excess scattering of the PEG solution with respect to the pure matched solvent can be attributed to incoherent scattering, which is fairly concentrated in the case presented here.

Figure 8b shows the excess scattering intensity (corrected for the incoherent background) of a mass fraction 1 % dendrimer solution in the matched solvent for PEG (filled circles), and of solutions at the same dendrimer concentration but this time in the presence of mass fraction 5 % PEG (squares) and mass fraction 15 % PEG (diamonds).

The highest PEG concentration studied by SANS was mass fraction 15 %. Samples at mass fraction (30 and 50) % were also prepared. However, these samples were highly turbid and seemed almost phase separated; they were highly viscous and did not equilibrate even after long stirring times (>50 h).

The data sets in Figure 8b could be satisfactorily fit to a Guinier functional form, yielding apparent radii of gyration equal to 40.0 Å ± 0.5 Å for the polymer free solution, 39.5 Å ± 0.5 Å for the mass fraction 5% solution and 39.8 Å ± 0.5 Å for the mass fraction 15 % PEG solutions. These results indicate that at these PEG concentrations, the dendrimers are reasonably well dispersed in the PEG solutions, since no significant upturn of the scattering is detected. Also, the dendrimer is not significantly affected by the presence of a relatively high concentration of neutral polymer. It appears that, in these conditions, the polymer surrounding the dendrimers does not exert an osmotic pressure sufficient to shrink the dendrimers.

Future Plans:

Dendrimers can be dispersed homogeneously in moderately high molecular weight PEG solutions (up to mass fraction 15 %), without any detectable variation of their radius of gyration. End-functionalized PEGwill be used to create polymer networks using the dendrimers as cross-linking points.

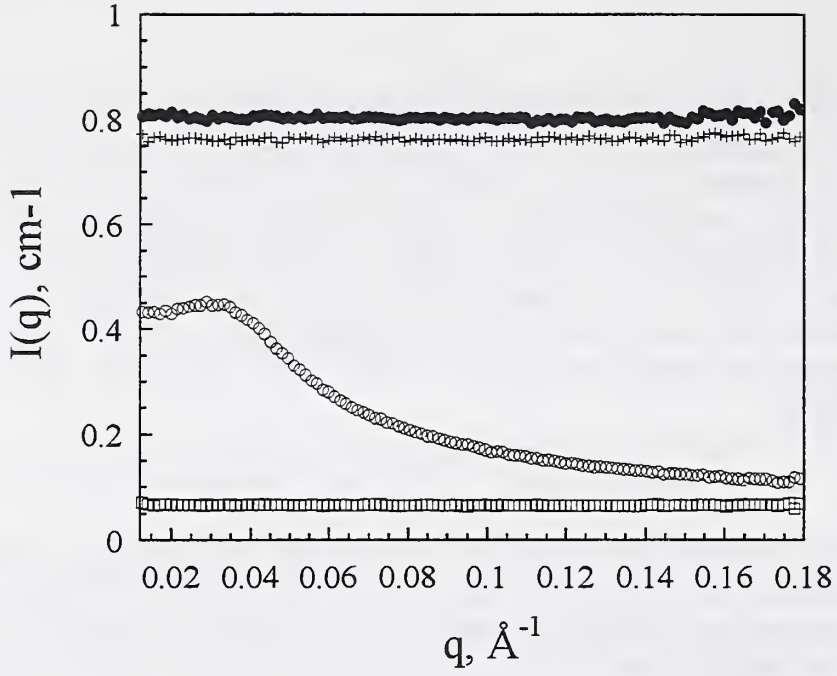

Figure 8a. Comparison of the scattering intensity of pure D_2O (squares), a mass fraction 15 % PEG solution in pure D_2O (open circles), the matched solvent (crosses) and a mass fraction 15 % PEG (filled circles) solution in the matching conditions.

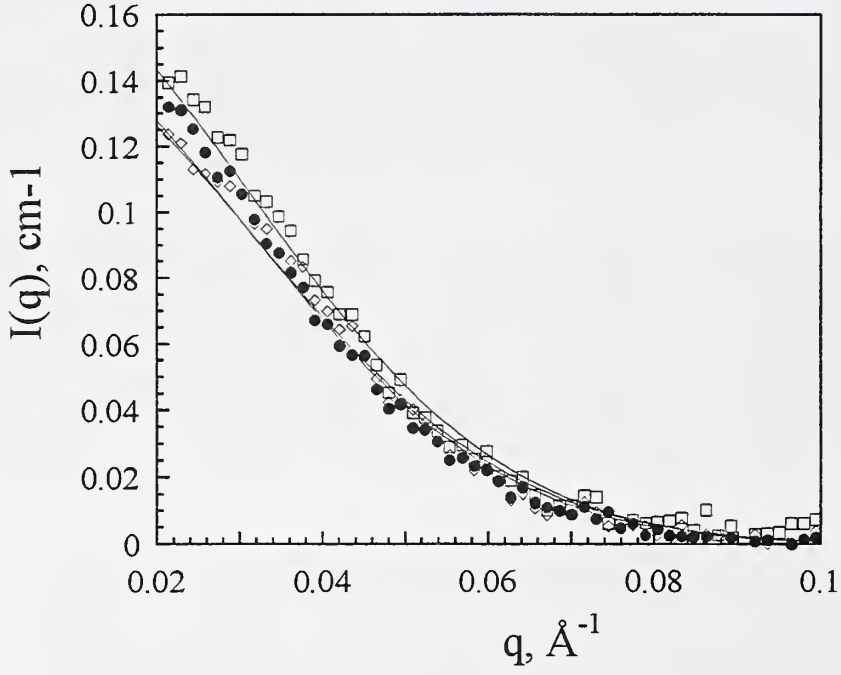

Figure 8b. Excess scattering intensity of a mass fraction 1 % dendrimer solution in the matched solvent for PEG (filled circles); solutions at the same dendrimer concentration but in the presence of mass fraction 5 % PEG (squares) and mass fraction 15 % PEG (diamonds).

Dendrimer Gold Colloids

NIST: Franziska Gröhn, Barry J. Bauer, Yvonne Akpalu, Catheryn L. Jackson, Eric J. Amis

Outside Collaborators: Donald Tomalia

Objectives:

To evaluate charged dendrimers as nanotemplates for the controlled formation of inorganic-organic hybrid colloids in aqueous solution.

Technical Description:

Synthesize gold nanoparticles within PAMAM dendrimers. Use small angle neutron Scattering, small angle x-ray scattering, and transmission electron microscopy (SANS, SAXS and TEM respectively) to study the influence of reaction speed, loading ratio and dendrimer generation on the structure of these gold containing dendrimers.

Summary Report:

$HAuCl_4$ is added to aqueous solutions of PAMAM dendrimers. After an equilibration time the reduction agent (sodium borohydride, $NaBH_4$, or hydrazine) is added. It turns out that a maximum ratio of 1:1 gold salt to dendrimer end groups can be added without precipitation. Reduction of the gold results in stable solutions of red-brown to red colloidal gold. Thus, the dendrimer stabilizes the gold colloid in aqueous solution. TEM and SAXS were performed on samples obtained under different reduction conditions such as reduction speed (as controlled by the pH of the solution) and ratio of gold to surface groups. TEM on the dendrimer-gold-nanoparticles is performed where the dendrimer is stained with phosphotungstic acid. Figure 9a shows an example of ≈4 nm gold-colloids within ≈13 nm G9-dendrimer. Under slow reduction conditions, well-defined metal colloids are formed. The radius of gyration obtained from SANS is the same as obtained for the plain dendrimer, showing that aggregation of the dendrimers avoided in solution.

SAXS data lead to more detailed information about the dendrimer-gold hybrid-particles. The scattering curve I(q) shown in figure 9b (corresponding to the TEM in figure 9a) can be Fourier transformed into the pair correlation function P(r) shown in figure 9c. The typical functional form of a layered sphere is found, with an inner sphere of ≈4 nm diameter and an outer sphere of ≈13 nm diameter corresponding well with the TEM results. However, the scattering curve and the P(r) function cannot be completely described when assuming spherical symmetry. By modeling it can be demonstrated that the gold particle is offset from the center of the dendrimer.

While for a ratio of gold to surface groups of 1:4 or 1:2 many small gold particles are formed in each dendrimer, for a ratio of 1:1, one gold particle per one dendrimer can be formed. For generations 6 to 9 the size of these gold colloids corresponds well with that expected by assuming all gold ions added per dendrimer form one particle (e.g 4 nm for 2064 atoms in the shown example). Interestingly, for G10 multiple smaller gold particles per dendrimer are observed under the same conditions.

Future Plans:

To make monolayers of the gold containing dendrimers and characterize them by x-ray reflectivity. Synthesize other inorganic colloids within the dendrimers. To make solid gold-dendrimer-polymer ternary composite materials.

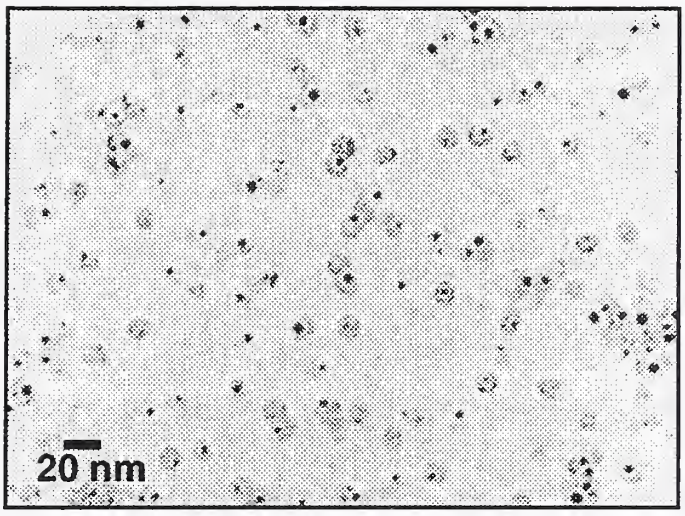

Figure 9a. TEM of gold containing G9 PAMAM dendrimer. The dendrimer is stained with phosphotungstic acid (dendrimer grey, gold black).

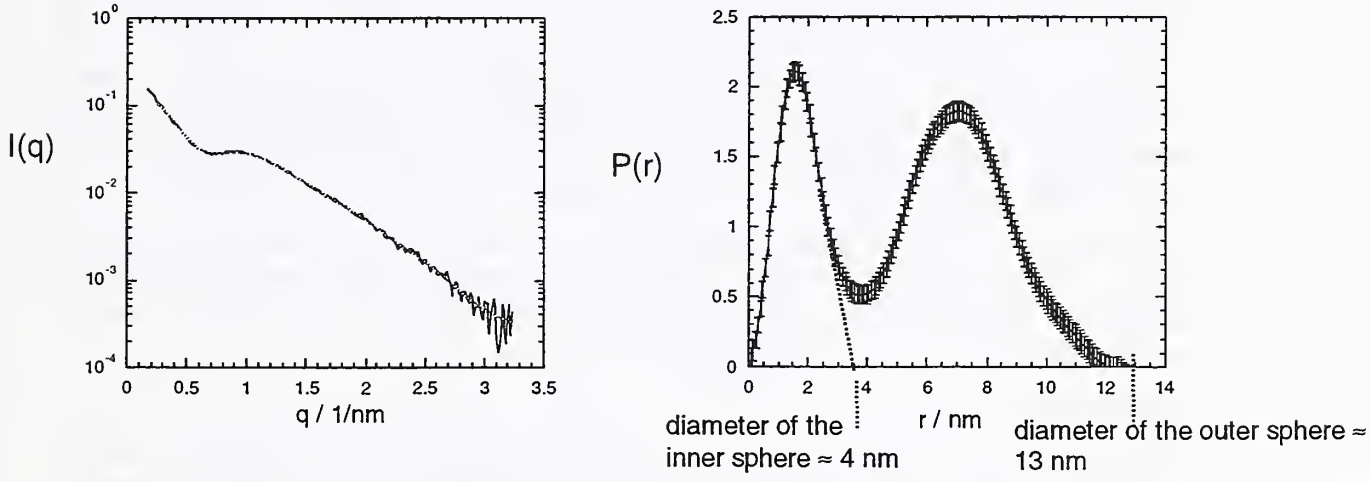

Figure 9b) Small angle x-ray scattering curve I(q) of the gold containing G9 PAMAM-dendrimer along with fit to the data, 9c) Pair distribution function P(r) obtained by inverse Fourier transformation of the scattering data I(q)

Gold Filled Fatty Acid Modified Dendrimers

NIST: Franziska Gröhn, Barry J. Bauer, Eric J. Amis

Outside Collaborators: Rolf Scherrenberg, DSM

Objectives:

To use hydrophobically modified dendrimers as "unimolecular micelles" in the preparation of dendrimer based nanocomposites.

Technical Description:

Form nanocomposites by reduction of gold salts in organic solutions of hydrophobically modified dendrimers. Characterize the resultant structures by TEM, SANS, and SAXS.

Summary Report:

A G5 fatty acid modified DSM dendrimer is dissolved in toluene at 55 °C. $HAuCl_4 \cdot 3H_2O$ is solubilized by the dendrimer as indicated by the yellow color of the solution. Reducing the gold salt results in stable red to violet solutions of colloidal gold in toluene.

The different steps of the synthesis are investigated by SANS and SAXS, as shown in figure 10a. While the plain dendrimer is a spherical molecule in solution, the gold-salt dendrimer complex forms cylindrical multi-dendrimer structures. The Fourier transformation of the scattering curve leads to a pair distribution function typical of cylinders. The obtained cross section density profile of the cylinders (figure 10b) is reasonable in terms of a swollen dendrimer core (radius ≈1.9 nm) plus fatty acid chains (≈1.3 nm). The cross section profile is further confirmed by the SAXS experiment on the same sample. Again, cylindrical structures are observed, but with a homogeneous cross section with a radius of ≈ 2 nm, since only the gold is seen in the x-ray scattering.

Reduction of the gold salt yields spherical gold particles. This may be understood by the density change of the gold with reduction. For all tested reducing methods, the gold colloids are bigger than expected when formed within one dendrimer, which also can be explained by an intermediate multi-dendrimer transition state.

Future Plans:

Study the influence of concentration and loading ratio on the structures formed by SAXS and SANS. Make more "controlled" gold colloids after understanding the phase behavior. Use the metal containing dendrimers as "markers," e.g. by incorporating them into polymer blends.

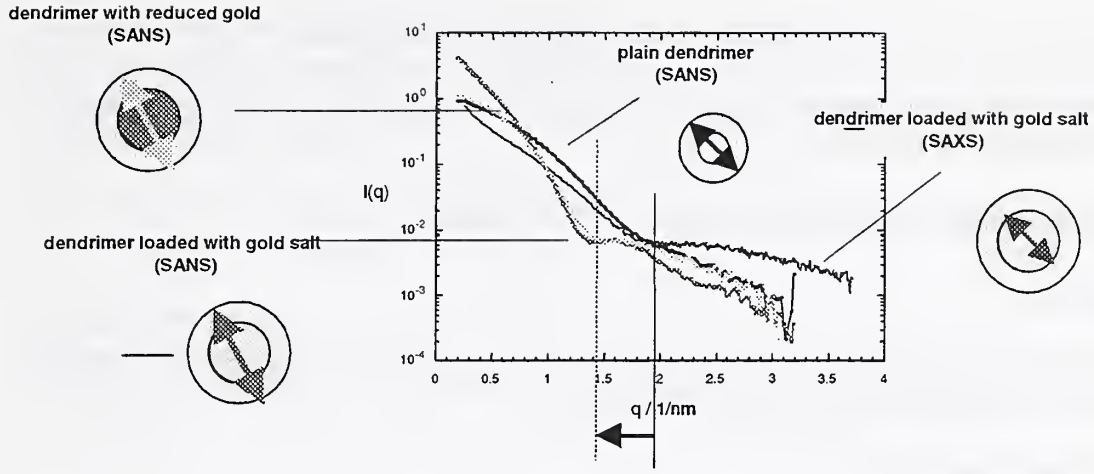

Figure 10a. SANS of the initial plain dendrimer, the dendrimer loaded with gold salt and the sample with reduced gold. For the dendrimer loaded with gold salt, the x-ray scattering curve is also shown.

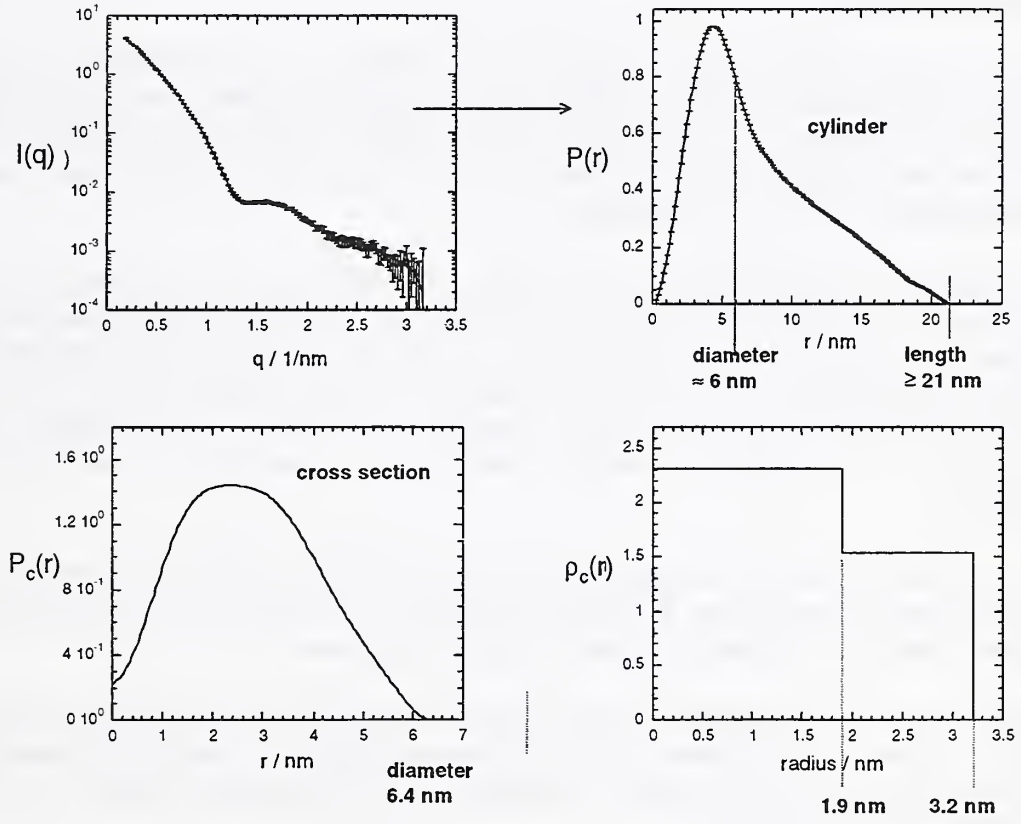

Figure 10b. Analysis of the SANS data for the dendrimer loaded with gold salt. Scattering curve I(q) with fit to the data, pair distribution function P(r). This is the typical function of a cylinder cross-section pair-distribution function obtained by inverse Fourier Transformation of the scattering data I(q) assuming cylindrical geometry with fit to the data, cross-section density profile ρ(r) obtained by deconvolution of the cross-section pair distribution function.

Dewetting of Hypergraft Thin Films

NIST: Kathleen A. Barnes, Alamgir Karim, Jack F. Douglas, Da-Wei Liu, Barry J. Bauer, Eric J. Amis

Outside Collaborators: Donald Tomalia, Rui Yin, MMI.

Objectives:

To measure the dewetting of hypergraft films and to estimate the effect of entanglements in the dendrigrafts as a function of generation

Technical Description:

Thin films of linear polymer and hypergrafts of various generations are spin cast from selective solvents on a flat substrate. The dewetting is followed through optical microscopy as a function of annealing time.

Summary Report:

We investigate the dewetting of entangled and unentangled polymer films from model polymer and inorganic substrates. Linear and hypergraft polyethyloxazoline (PEOX) polymers are chosen as the unentangled and entangled dewetting fluids, respectively. Spin cast films of approximately 50 nm were cast on polystyrene coated silicon wafers and annealed at 130 °C for various times.

Holes nucleate at random positions in the film and slowly grow in the early stage of dewetting. This early-stage dewetting is found to be similar in entangled and unentangled polymer films and to be largely independent of substrate. Figure 11a is a micrograph of an intermediate stage of dewetting of an entangled G2 PEOX (Image width is 90 μm in all figures). Unconventional deweting pattern can be seen with inhibited hole coalescence. A foam-like "network" is formed that has uniform cell size and wall thickness.

Figure 11b shows late stage dewetting of the same G2 PEOX. Relatively uniform droplet coverage and size results that is formed by break-up of fluid walls and retraction into droplets. There is no further significant evolution of structure.

Figure 11c shows a micrograph of the late stage dewetting of a G0 (conventional graft) PEOX. A conventional cellular pattern is formed that has been observed previously for low molecular weight linear chains. Therefore, a lightly branched polymer acts in a similar way to linear polymer.

Late-stage dewetting in the entangled films is significantly different because of the inhibition of hole coalescence in the intermediate stage of film dewetting. The holes in the entangled film continue to grow in size until they impinge on each other to form a foam-like structure with a uniform "cell" size. The boundaries of these cells break-up and retract to the vertices of the former cellular network to form a relatively uniform

droplet configuration. In contrast, there is substantial hole coalescence in the unentangled polymer films in intermediate-stage of dewetting that leads to large and polydisperse hole patterns. Thus, entanglement has a large influence on the final morphology of dewetted polymer films.

This suggests that hypergraft polymers of high generation entangle to a much greater extent than linear polymers.

Future Plans:

To follow the dewetting of linear films placed on dendrimer coated substrate.

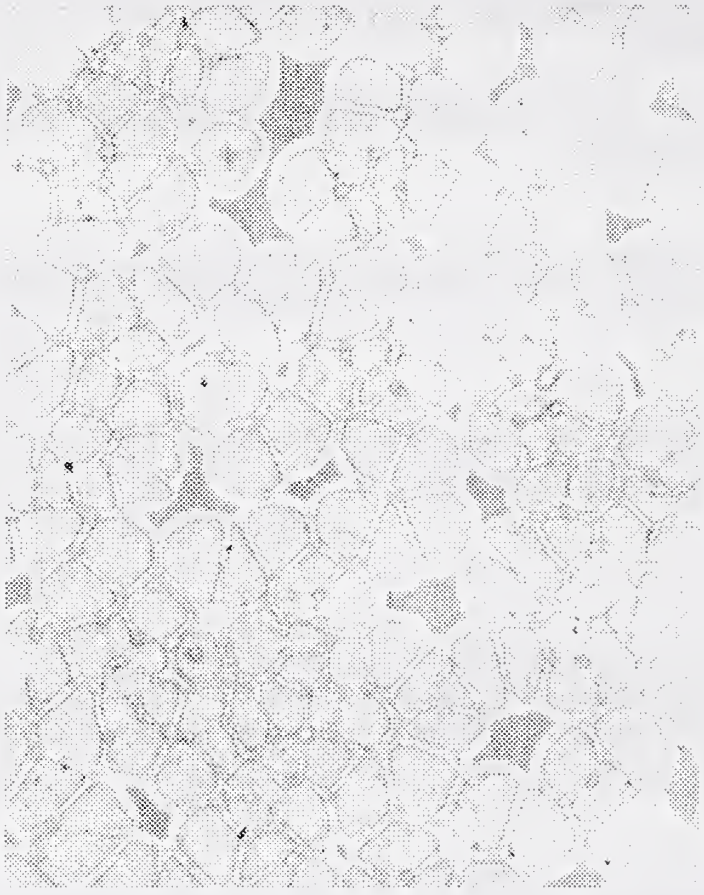

Figure 11a. Intermediate stage dewetting of entangled G2 PEOX on a polystyrene substrate

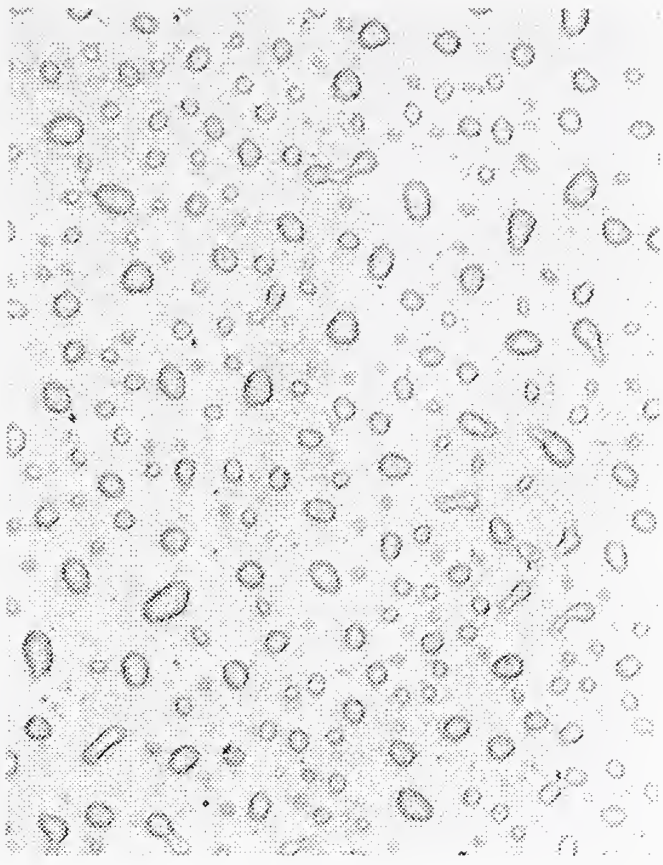

Figure 11b. Late stage dewetting of entangled G2 PEOX on a polystyrene substrate

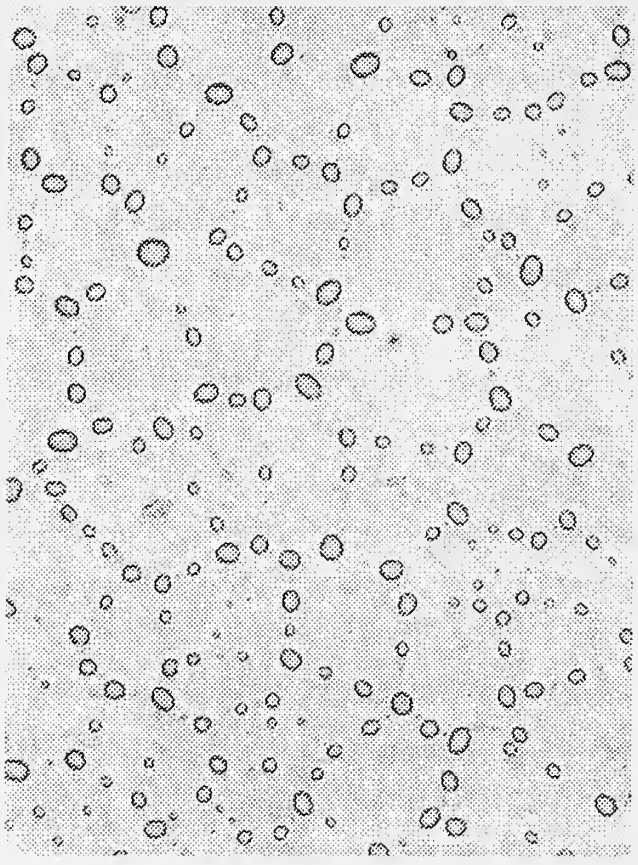

Figure 11c. Late stage dewetting of unentangled G0 PEOX on a polystyrene substrate